Supporting Information

Appendix

Mapped Coral Mortality and Refugia in an Archipelago-scale Marine Heatwave

Gregory P. Asner[1*], Nicholas R. Vaughn[1], Roberta E. Martin[1], Shawna A. Foo[1], Joseph Heckler[1], Brian J. Neilson[2], Jamison M. Gove[3]

[1]Center for Global Discovery and Conservation Science, Arizona State University, Hilo HI 96720

[2]Division of Aquatic Resources, Department of Land and Natural Resources, Honolulu HI 96813

[3]Pacific Islands Fisheries Science Center, National Oceanic and Atmospheric Administration, Honolulu, HI 96818

*Correspondence to: Greg Asner, gregasner@asu.edu, Tel: 1-808-757-9194

This file includes:
Methods
Figs. S1-S4
Tables S1-S4
SI References

Methods

Airborne data collection

During the 2019 and 2020 airborne campaigns, the Global Airborne Observatory (GAO) recorded data from two coaligned instruments: a high-fidelity visible-to-shortwave infrared (VSWIR) imaging spectrometer and a light detection and ranging (LiDAR) scanner (1). In addition, a 60 megapixel digital mapping camera was used to assess and manage sea surface glint levels during flight. A precise position and orientation system enabled the post hoc computation of aircraft trajectory to within 5 cm (RMSE) during all flights. Global Positioning System (GPS) timing data recorded by all three instruments allowed precise back-computation of position and orientation for the receiver of each instrument. Airborne operations were performed from 0830-1100 local time to optimize scene lighting and minimize wind conditions. Nominal flight altitude was 2 km above the sea surface and flightlines were spaced to achieve 50% overlap in VSWIR spectrometer coverage. Aircraft groundspeed was maintained at 130-140 kt. LiDAR pulse frequency was set to 200 kHz and scan frequency was 34 Hz with a field of view of 38°, allowing 2° of buffer on each side of the spectrometer field of view of 34°. Under these conditions, nominal pulse density is more than 4 pulses m^{-2}, sufficient to retrieve a sufficient map of the sea surface height during the time of flight.

Data processing

Data from all three GAO instruments were orthorectified, and the spectrometer data were radiometrically and atmospherically corrected using the same methodology used to generate 2019 maps (2). In summary, the raw LiDAR point cloud data were first converted to a 1 m resolution digital surface model (DSM) by interpolating between the first returns from each pulse. The raw VSWIR spectrometer data collected onboard the GAO were first converted to 427-band radiance in the 350-2500 nm wavelength range using a laboratory-based calibration. The known orientation of the spectrometer was used with the LiDAR DSM to retrieve the three-dimensional (sea level) position of each spectrometer pixel. Using the LiDAR-derived observation angles and elevation as inputs, we performed atmospheric correction with a modified version of the ATREM model (3, 4). Orthorectification of each flight line was adjusted for water refraction and depth.

A neural network deep learning model (5) was applied to compute depth for each flight line, which was used to ray trace a refraction-corrected pixel location on the seafloor. With the location of each spectrometer pixel known, individual flight lines were mosaicked together using a strategy of minimum glint, where glint is computed using the average reflectance value for the five spectral bands covering 890-910 nm for each pixel. For each mosaic map pixel location, data from the flight line with the lowest glint at that location was kept.

Live coral mapping

The initial percent live coral cover estimates for 2019 were taken from previously produced maps produced in an earlier study, where data from GAO spectrometer reflectance maps were used to train a neural network model designed to partition cover into four classes: sand, live coral, algae, and rock (2). All depth values in this analysis were generated using the existing

depth model and a flight line averaging approach (6) applied to all 2019 and 2020 reflectance data to get the best estimate for each given location.

To be able to detect change in coral cover between 2019 and 2020, predicted cover values from the 2019 live coral cover maps were incorporated into the training data to standardize live coral cover estimates in 2020 data. This was done in a sectional manner by first partitioning all covered Hawaiian coastlines into 10 km stretches and then training a separate model for each 10-km section on the 2020 GAO reflectance values.

For each of these sectional models, a training data set was compiled using the 37,378 points collected in the 2019 campaign combined with 15,000 pixels from the 2019 cover maps within the coastline segment region. Pixels were selected from the full 10-km area of coastline buffered by 0.04° (approx. 4.2-km) on each end, and a pixel selection design was created to ensure that selected training pixels portrayed the full range of possible values for live cover, sand cover, and depth. Under this design, an equal number of samples were taken from each combination of a grid defined by three variables binned as: (i) 2019 live coral cover broken into five bins defined [0%, 20%, 40%, 60%, 80%, 100%], (ii) 2019 sand cover broken into five bins defined [0%, 20%, 40%, 60%, 80%, 100%], and (iii) benthic depth broken into seven bins defined [0m, 2m, 5m, 10m, 15m, 22m, 30m, ∞]. Each sectional neural network model used the same initial design, except that the number of total nodes could vary to minimize overfitting. The neural network model input layer contained benthic depth, estimated glint level (computing using NIR reflectance as defined above), and 55 spectral reflectance bands from 420-690 nm. Prior to input into the model, reflectance data were pretreated by smoothing and pinning. The smoothing operation used a gaussian kernel with a width of seven bands and a standard deviation of three bands. After smoothing, all spectra were pinned such that the reflectance value at 420 nm was subtracted from the reflectance value for all other bands within the spectrum. In this way, the original value at 420 nm was retained to provide the model with information about pixel brightness, while the values for following wavelengths were now relative to this brightness at 420 nm. This generated smaller standard deviations for each input wavelength across all samples. Given a starting number of hidden layer nodes, N, the full neural network model structure was sequentially defined as:

1. Input layer – 57 nodes
2. Batch Normalization layer
3. Hidden dense layer – N nodes, Rectified Linear Unit (ReLU) activation function
4. Dropout operation – dropout proportion = 0.2
5. Hidden dense layer – 0.75 x N nodes, ReLU activation
6. Dropout operation – dropout proportion = 0.2
7. Hidden dense layer – 0.5 x N nodes, ReLU activation
8. Output layer – 4 nodes (Sand, Live coral, Algae, Rock), sigmoid activation (meaning the value of each node is restricted to the range [0-1])

The value for the number of nodes (N) was initially set to 400 for each 10 km coastal region, and a 5-fold cross validation approach was used to calculate a predicted class for each training pixel using a model not trained with that pixel. The ADAM optimizer (7) was used for model optimization and a MSE loss function was used. An observed and predicted dominant class was determined by selecting the class with the highest cover value for each pixel, and a kappa

statistic was computed for the confusion matrix built with all samples in the training data set. Each model was then iteratively refit as N was dropped by 25% at each iteration. If a kappa value of at least 0.5 was achieved during any iteration, then the iteration stopped when the kappa value dropped by more than 0.05 from the largest observed kappa value. Reducing N often improved the model fit compared to models with more nodes or when N dropped below a minimum of 28, and the previous model was retained for this section. If no kappa > 0.5 was found during iteration, it was due to lack of variation in one or more classes, and we used the original 2019 proportional cover model to estimate the 2020 cover values for this coast section. From applying the final model to the 2020 reflectance maps for each coastal section, we produced a 2020 live coral cover map for each section. We created 2020 maps for each island by mosaicking the individual coastal maps together at 2 m resolution. We generated maps of estimated loss of live coral cover as the pixel-level change in live coral cover (%) in each 2 m pixel, which was calculated as the difference in percent live coral cover between the two years.

Comparisons of remote sensing and field estimates

We carried out diver-based transect surveys to assess error in our remotely sensed live coral cover estimates. At each site, we installed a 25-m transect at three isobaths of 5, 10 and 15 m depth. Divers recorded benthic composition every 0.25 m to species level for living taxa and recorded all non-living substrate. GPS coordinates were taken at the start and end of each transect. An Arizona State University (ASU) set of 129 transects on Hawai‘i Island had a depth breakdown of < 5 m (n = 2), 5-10 m (n = 48), 10-15 m (n = 49), and > 15 m (n = 30). The Hawai‘i Department of Land and Natural Resources, Division of Aquatic Resources (DAR) collected similar transects at depths ranging from < 5 to > 15 m on the islands of Hawai‘i (n = 28), Maui (n = 297), Moloka‘i (n = 29), and O‘ahu (n = 649). The depth breakdown of the DAR data was < 5 m (n = 763), 5-10 m (n = 153), 10-15 m (n = 86), and > 15 m (n = 1). Combined, the ASU and DAR data totaled 1132 transects on four islands. Results indicate high precision (R^2 = 0.94) and accuracy (RMSE = 7.7%) between airborne and field-based estimates of live coral cover (**Fig. S3**).

We also assessed the relationship between field-estimated coral bleaching during the 2019 marine heatwave and spectroscopy-based coral mortality following the heatwave. Coral bleaching data were provided by Winston et al. (8). While gross rates of bleaching and net rates of mortality do not represent the same measure of coral resilience, comparison indicates how well the two processes relate during versus after the heatwave. We found that mortality accounted for about 78% of the measured coral bleaching at the transect or site scale (**Fig. S4**). Importantly, these results only indicate site-level relationships, suggesting that about 22% of sites that bleached subsequently had some recovery. Within-site (coral-scale) relationships were not tested due to the approximate locations (with > 10 m GPS error) of the coral bleaching transects.

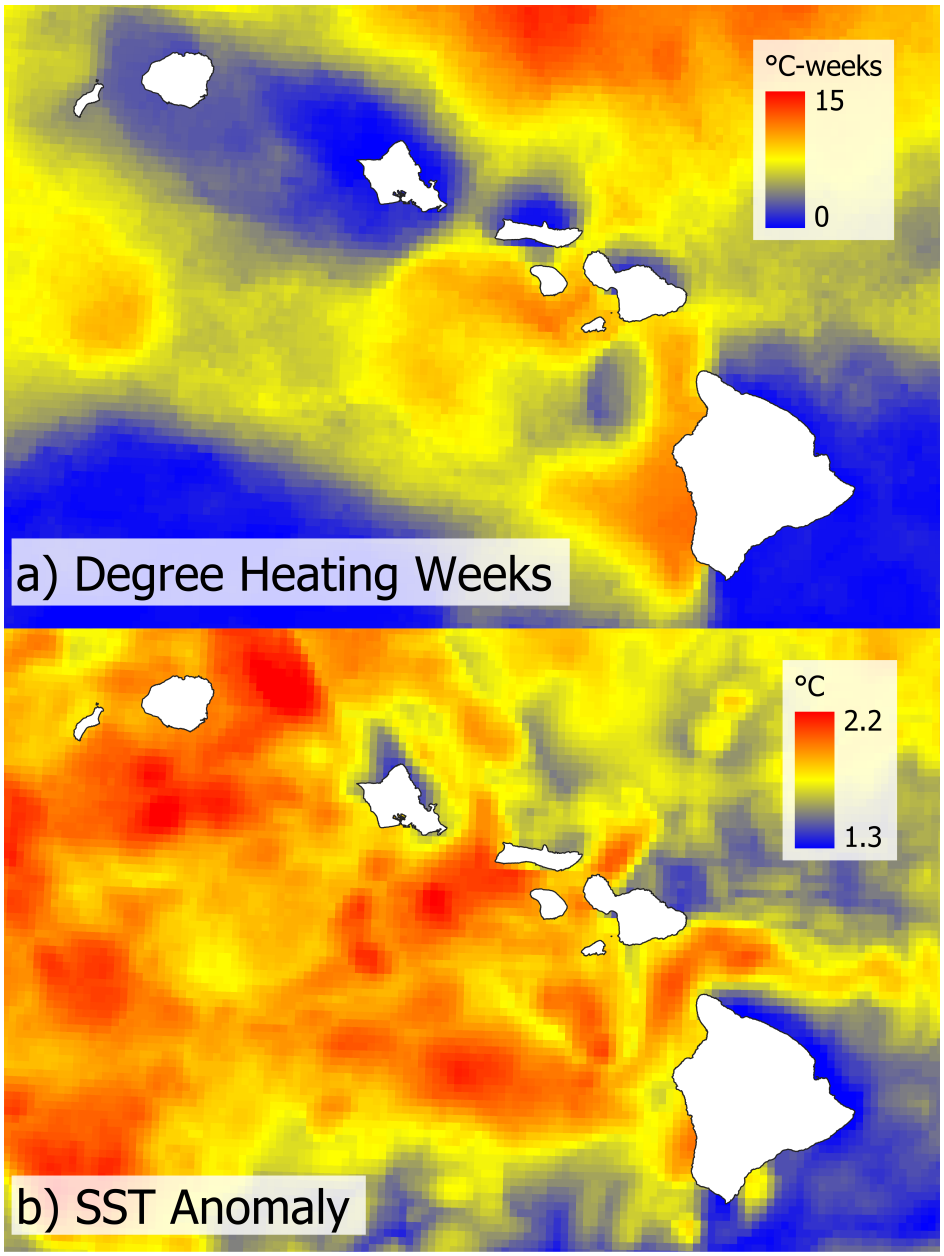

Fig. S1. (a) Degree heating weeks and (b) sea surface temperature (SST) anomaly maps for the Main Hawaiian Islands during the 2019 (July-October) marine heatwave. Source: NOAA Coral Reef Watch

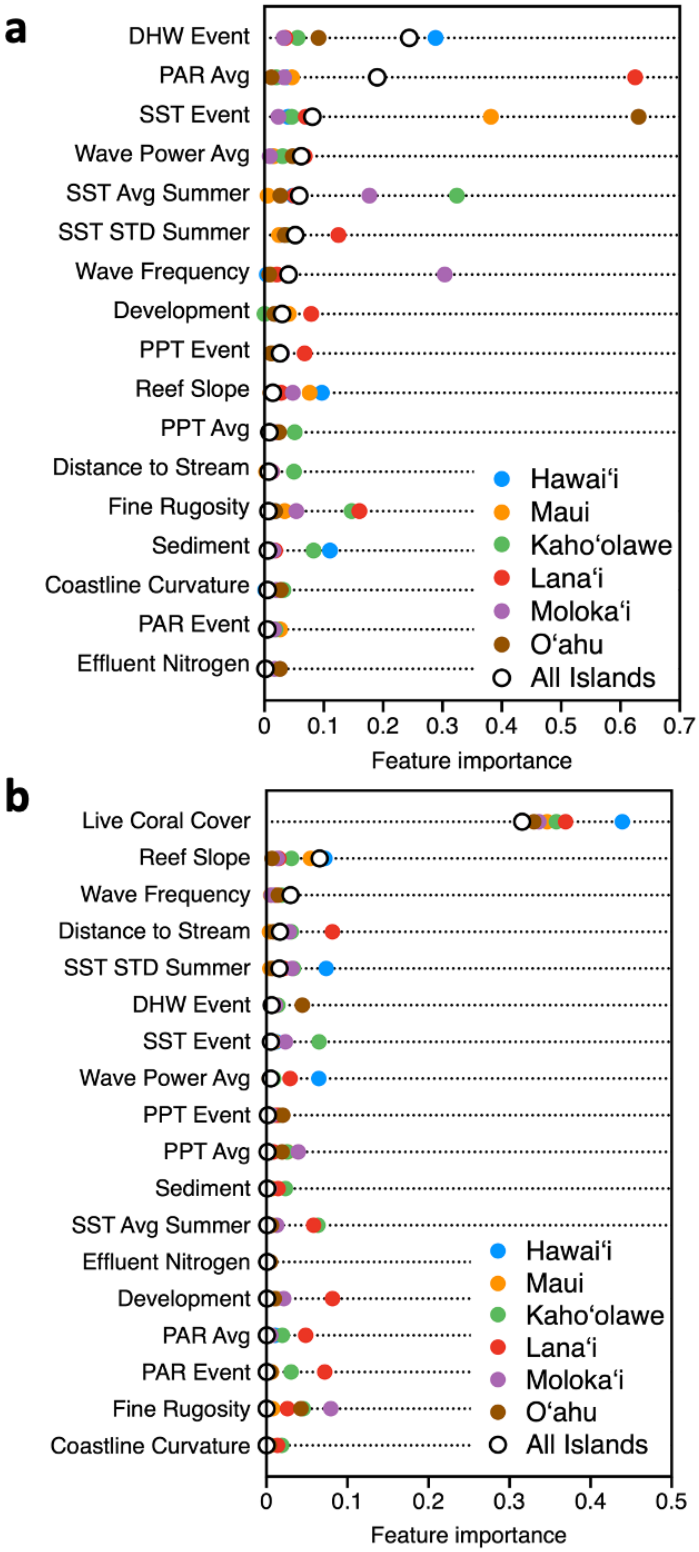

Fig. S2. Importance of factors associated with the spatial distribution of **(a)** absolute and **(b)** relative coral loss for each island following the 2019 marine heatwave in the Hawaiian Islands.

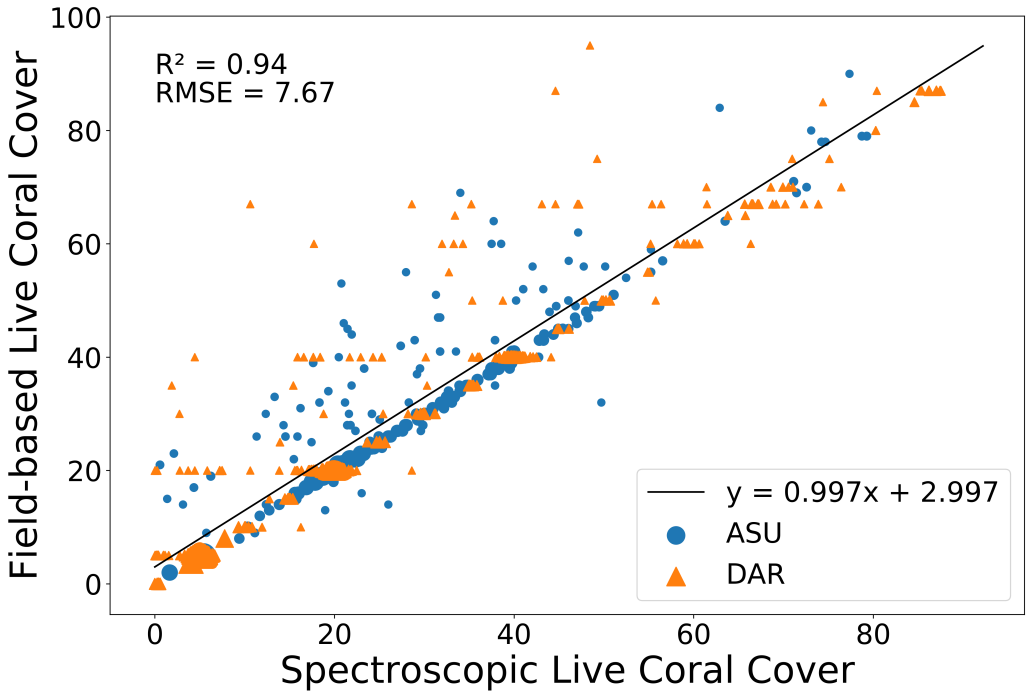

Fig. S3. Field verification of airborne live coral cover mapping across four Hawaiian Islands (n = 1132 transects) during the marine heatwave.

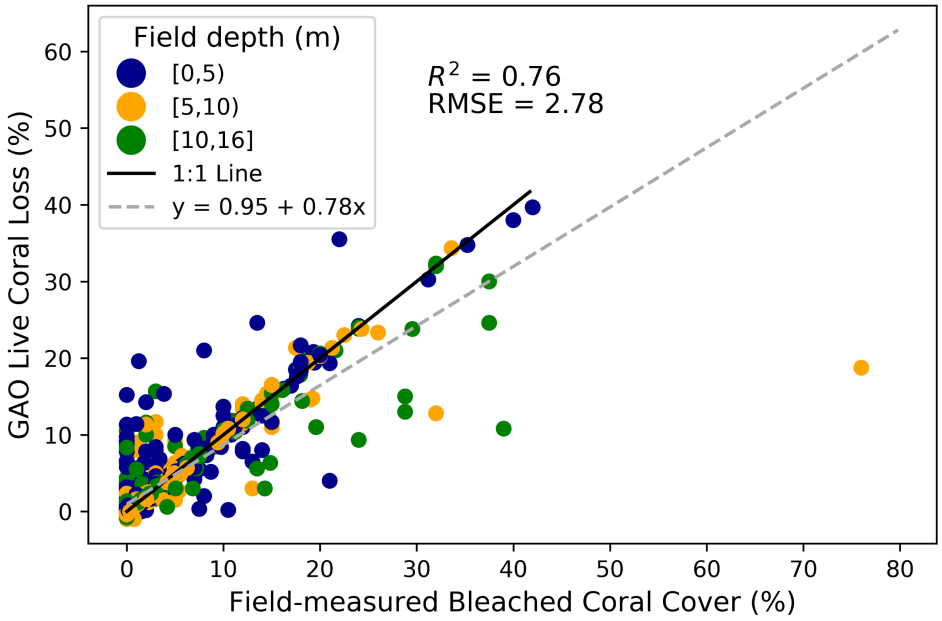

Fig. S4. Comparison of field-estimated coral bleaching during the 2019 marine heatwave (8) and post-heatwave coral mortality from airborne mapping.

Table S1. Mapped human and environmental factors used in the island-scale Random Forest Machine Learning (RFML) analyses of coral mortality from 2019 to 2020 as well as the assessments of driver correlates with potential coral refugia.

Name	Description	Source	Units	Native Res.
GAOFineRug	Fine rugosity	GAO [2,5,6]	--	2 m
GAOSlope	Slope	GAO [2,5]	--	10 m
CLineCurv	Coastline complexity	HI OP[a]	m	--
BayDist2k	Distance inside embayment	HI OP[a]	m	--
BayPos2k	Embayment head-shoulder position	HI OP[a]	--	--
StreamDist	Distance to stream	HI OP[a]	m	--
MeanPAR	Mean PAR 2013-2019	NOAA[b]	Einstein m^{-2}	750 m
MHIPAR	Mean PAR Aug-Dec 2019	NOAA[b]	Einstein m^{-2}	750 m
WarmingDHW	Degree heating weeks Aug-Dec 2019	NOAA[b]	°C wk	0.05°
WarmingSST	Average SST Aug-Dec 2019	NOAA[b]	°C	0.05°
SST	Average summer SST 2013-2019	NOAA[b]	°C	0.05°
SSTSTD	Standard deviation summer SST 2013-2019	NOAA[b]	°C	0.05°
Prcp2019	Total rainfall 2019	NASA[c]	mm	0.1°
PrcpEvent	Total rainfall Aug-Dec 2019	NASA[c]	mm	0.1°
OTPEffN	Nitrogen Flux	OTP [8]	kg km^{-2} d^{-1}	0.005°
OTPWaveFreq	Anomalous wave frequency	OTP [15,17]	Count yr^{-1}	0.005°
OTPWaveAvgP	Average hourly maximum wave power	OTP [15,17]	kW m^{-1}	0.005°
OTPDevel	Nearshore development index	OTP [15,20]	--	0.005°
OTPSedmnt	Total effluent	OTP [15]	gal km^{-2} d^{-1}	0.005°

[a]Derived from coastline data available at https://planning.hawaii.gov/gis

[b]From daily VIIRS chlorophyll and PAR data downloaded from Coral Reef Watch https://coralreefwatch.noaa.gov/product/oc/hawaii_main.php

[c]From daily GPM rainfall maps downloaded from NASA https://gpm1.gesdisc.eosdis.nasa.gov/data/GPM_L3

Table S2. Random Forest Machine Learning (RFML) model results and optimal meta parameters for archipelago and island scales. Absolute loss is the change in percentage cover of live coral between years, and relative loss is calculated as [2019-2020]/2019.

Region	Loss Type	R^2	Estimators	Max. Depth	Min. Samples
--Archipelago scale--					
All islands	Absolute	0.31	250	5	2
	Relative	0.34	50	5	5
--Island scale--					
Hawai‘i	Absolute	0.33	500	5	10
	Relative	0.51	100	5	5
Maui	Absolute	0.31	5000	5	2
	Relative	0.35	100	5	10
Kaho‘olawe	Absolute	0.64	100	5	5
	Relative	0.66	100	5	2
Lana‘i	Absolute	0.71	250	5	2
	Relative	0.46	250	5	2
Moloka‘i	Absolute	0.45	5000	5	2
	Relative	0.39	100	5	5
O‘ahu	Absolute	0.32	250	5	5
	Relative	0.39	100	5	5

Table S3. Top ten highest live coral cover reefs identified in (2).

Rank	Name	Longitude	Latitude	Area (ha)	2019 Starting Live Cover (%)
1	Hawai‘i - Kīholo	-155.93	19.86	98.8	35.2 (16.1)
2	Hawai‘i - Keawaiki	-155.91	19.89	17.1	34.5 (15.0)
3	Hawai‘i - ‘Anaeho‘omalu	-155.90	19.91	71.9	29.9 (15.3)
4	Hawai‘i - Keaukaha	-155.05	19.73	24.5	38.3 (21.6)
5	Hawai‘i - Pāpā Bay	-155.90	19.21	7.9	32.6 (10.1)
6	Lana‘i – East	-156.80	20.82	175.9	50.2 (25.2)
7	Hawai'i - Makako	-156.06	19.73	18.5	26.5 (16.6)
8	Maui - Kaanapali South	-156.69	20.91	29.4	32.4 (20.4)
9	Moloka‘i - SE	-156.92	21.04	422.1	39.6 (24.2)
10	Hawai‘i – Wai‘olena	-155.02	19.73	0.2	32.6 (11.6)

Table S4. Details on potential reef refugia, relative coral loss from 2019 to 2020, and environmental factors for each refugium and surrounding reefs (see Table S3). Units for these factors are provided in Table S1. Raw cover loss values for each reef are given in Table 2.

Rank	Island	Reef	Relative Loss (%)		SST		SSTa		DHW		Mean PAR		Wave Power		Wave Frequency		Reef Slope		Land Development		Sedimentation		Effluent	
			Refuge	Surrounding	Refuge	Surrounding	Refuge	Surrounding	Refuge	Surrounding	Refuge	Surrounding	Refuge	Surrounding	Refuge	Surrounding	Refuge	Surrounding	Refuge	Surrounding	Refuge	Surrounding	Refuge	Surrounding
1	Hawaii	Kiholo	18.1	27.4	28.8	28.8	1.81	1.80	10.2	10.3	0.090	0.073	1.97	3.61	0.054	0.050	2.0	2.1	0.002	0.015	0.0	0.2	108	80
2	Hawaii	Keawaiki	19.4	27.6	28.8	28.8	1.81	1.81	10.1	10.2	0.074	0.073	2.63	3.12	0.048	0.049	4.0	2.2	0.005	0.012	0.0	0.6	52	113
3	Hawaii	ʻAnaehoʻomalu	19.4	27.6	28.8	28.7	1.80	1.80	10.2	10.0	0.075	0.072	2.66	2.93	0.047	0.048	2.6	2.1	0.004	0.011	0.0	0.6	34	119
4	Hawaii	Keaukaha	17.4	29.0	27.7	27.7	1.27	1.28	0.4	0.5	0.109	0.087	7.55	16.86	0.129	0.131	3.0	3.0	0.145	0.054	0.0	0.4	3132	383
5	Hawaii	Pāpā Bay	27.6	41.5	28.8	28.8	1.97	1.92	11.8	11.5	0.063	0.064	5.77	7.42	0.056	0.057	9.6	2.0	0.032	0.019	0.0	0.0	948	52
6	Lanai	East side	26.8	28.6	28.6	28.6	1.91	1.88	9.1	8.3	0.084	0.067	2.58	3.59	0.179	0.185	3.1	2.0	0.003	0.012	9.8	0.9	0	116
7	Hawaii	Makako	31.4	29.1	28.7	28.8	1.74	1.78	10.7	10.7	0.069	0.068	4.14	4.85	0.049	0.055	9.7	1.8	0.064	0.018	0.0	0.0	84	326
8	Maui	Kaʻanapali South	25.5	27.6	28.5	28.4	1.87	1.85	8.3	7.4	0.063	0.070	2.00	6.23	0.178	0.168	2.4	2.0	0.128	0.018	14.5	1.2	2329	202
9	Molokai	Southeast side	20.0	31.8	28.2	28.2	1.72	1.74	2.1	3.3	0.075	0.073	1.08	10.87	0.071	0.160	3.1	2.0	0.002	0.003	5.3	0.7	735	103
10	Hawaii	Wai'olena	19.9	28.7	27.7	27.7	1.26	1.28	0.4	0.5	0.102	0.085	12.45	16.80	0.131	0.131	2.7	3.0	0.151	0.060	0.0	0.4	435	371

SI References

1. G. P. Asner *et al.*, Carnegie Airborne Observatory-2: Increasing science data dimensionality via high-fidelity multi-sensor fusion. *Remote Sensing of Environment* **124**, 454-465 (2012).
2. G. P. Asner *et al.*, Large-scale mapping of live corals to guide reef conservation. *Proceedings of the National Academy of Sciences* **117**, 33711-33718 (2020).
3. B.-C. Gao, A. F. H. Goetz, Column atmospheric water vapor and vegetation liquid water retrievals from Airborne Imaging Spectrometer data. *Journal of Geophysical Research* **95** (1990).
4. D. R. Thompson *et al.*, Airborne mapping of benthic reflectance spectra with Bayesian linear mixtures. *Remote Sensing of Environment* **200**, 18-30 (2017).
5. G. P. Asner, N. R. Vaughn, C. Balzotti, P. G. Brodrick, J. Heckler, High-Resolution Reef Bathymetry and Coral Habitat Complexity from Airborne Imaging Spectroscopy. *Remote Sensing* **12** (2020).
6. G. P. Asner *et al.*, Abiotic and Human Drivers of Reef Habitat Complexity Throughout the Main Hawaiian Islands. *Frontiers in Marine Science* **8** (2021).
7. B. J. A. Kingma DP (2014) A Method for Stochastic Optimization. (arXiv [cs.LG]).
8. M. Winston *et al.*, Preliminary Results of Patterns of 2019 Thermal Stress and Coral Bleaching Across the Hawaiian Archipelago. (2020).